

Journal of University of Babylon, Engineering Sciences, Vol.(26), No.(3): 2018.

The Effect of Adding Alloying Element Yttrium and Tantalum on Mechanical Properties of NiTi Shape Memory Alloy

Abdulkareem Abdulrazzaq Alhumdany

Mechanical engineering department, University of kerballa

Alhumdany@yahoo.com

Abdulraheem K. Abidali

College of Materials Engineering, Metallurgical department, University of Babylon

Abidalieng@yahoo.com

Hanan J. Abdulredha

Mechanical engineering department, University of kerballa

hananj@yahoo.com

Abstract

Nickel titanium (NiTi) shape memory alloys have increased utilization for different engineering applications especially in biomedical applications. The aim of this study, first studied the powder metallurgy process variables such as compacting stress and sintering cycles on several physical tests such as x-ray diffraction, porosity and apparent density as well as mechanical tests such as microhardness, surface roughness, second studied the effect of alloying element of yttrium and tantalum on microhardness, surface roughness of NiTi shape memory alloys. Several alloys have been prepared by powder metallurgical technique. Vickers hardness, surface roughness measurements, XRD analysis, porosity and apparent density were performed.

It was shown that the XRD diffraction tests of all samples have the same results of two phases at room temperature (RT) (monoclinic NiTi and hexagonal Ni₃Ti). the result of adding tantalum in the percentage of (1%, 2% and 3%) in the expense of nickel, increasing hardness value gradually to record the highest value (310) HV at 3% and also decrease the surface roughness from (0.36 to 0.15) μm at 3% Tantalum and 650 Mpa. While the result of adding yttrium in the percentage of (1%, 2% and 3%) % Wt. in the expense of nickel, shown that the specimen of 2 % Yttrium and 650 Mpa compacting stress showed the hardness value of (275.7) HV

The hardness value decreases at 3 % and 1% additives at the same compacting stress to (272.26 and 200) HV respectively. The addition of Tantalum element decreases the surface roughness from (0.36 to 0.15) μm at 3% Tantalum and 650 Mpa. While the specimen of 2% Yttrium at 650 Mpa shown (0.16) μm surface roughness.

Keywords: Nickel Titanium (NiTi); Superelasticity; Shape Memory Effect SME; XRD; Microhardness; Surface roughness.

الخلاصة

لقد زاد استخدام سبائك الذاكرة (النكل - تيتانيوم) في التطبيقات الهندسية المختلفة وكذلك في التطبيقات الطبية الحيوية. وكان الهدف من هذه الدراسة اولاً دراسة تأثير اختلاف ضغط الكبس ودورات التليد على عدة اختبارات فيزيائية مثل الأشعة السينية، والمسامية والكثافة الظاهرية، فضلاً عن الاختبارات الميكانيكية مثل ميكروهاردنيس، خشونة السطح، وثانياً دراسة تأثير عناصر السبك من الإيتريوم والتنتالوم على ميكروهاردنيس و خشونة السطح للسبائك المتذكّرة للشكل. وقد تم تحضير عدة سبائك بواسطة تقنية مساحيق المعادن. تم إجراء صلادة فيكرز، قياسات خشونة السطح، تحليل حيود الأشعة السينية، المسامية والكثافة الظاهرية. وقد تبين أن اختبارات حيود الأشعة السينية لجميع العينات لها نفس النتائج من الطورين في درجة حرارة الغرفة هما (NiTi و Ni₃Ti سداسي الشكل). أظهرت عينة ذات النسبة 2% الإيتريوم والمكبوسة تحت ضغط 650 ميغا باسكال قيمة صلابة (275.7). أما قيمة صلابة العينات ذو النسب 3% و 1% هي (272.26 و 200) ميغا باسكال قيمة صلابة (275.7). في حين إضافة التنتالوم يزيد من الصلادة تدريجياً ليسجل أعلى قيمة صلادة (310) عند 3%.

ان اضافة عنصر التنتالوم يقلل خشونة السطح من ٠.٣٦ إلى ٠.١٥ ميكرون بالنسبة للعينة ذات النسبة ٣٪ التنتالوم والمكبوسة تحت الضغط ٦٥٠ ميجا باسكال. في حين أن العينة ذات النسبة ٢٪ الإيتريوم المكبوسة تحت نفس الضغط أظهرت (٠.١٦) ميكرون خشونة السطح.

الكلمات المفتاحية: نيكل تيتانيوم ، المرونة ، ذاكرة الشكل ، حيود الاشعة السينية ، الصلادة ، خشونة السطح.

1. Introduction

Shape memory alloys (SMAs) based on Nickel Titanium were the alloys most frequently used in commercial applications because they combine good mechanical properties, wear resistant, biocompatibility, and the phenomenon of super-elasticity with shape memory effect (TARNIȚĂ *et.al.*, 2009). The biocompatibility of these alloys is one of the important points related to their biomedical applications as orthopedic implants, cardiovascular devices, and surgical instruments, as well as orthodontic devices (Mantovani, 2000). This study presents their main applications in the biomedical field as orthopedic devices (spinal vertebral spacer).

Shape memory alloys presents two well-defined crystallographic phases, i.e., austenite and martensite (OTSUKA and REN, 1999). Martensite was a phase that, in the absence of stress was stable only at low temperatures; in addition, it can be induced by either stress or temperature. Martensite can be easily deformed, reaching large strains (~8%) (DUERIG *et.al.*, 1999). Martensitic transformation explains the shape recovery in SMA. Four characteristic transformation temperatures can be defined: Ms and Mf (the temperatures at which the formation of martensite starts and ends), and As and Af (the temperatures at which the formation of austenite starts and ends) as shown in Fig. (1).

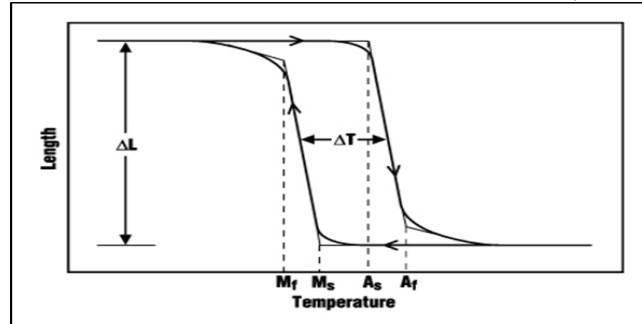


Fig. (1): the typical temperature-transformation curve of a NiTi alloy ((DUERIG, *et.al.*, 1999): Ms: martensite start temperature upon cooling; Mf: martensite finish temperature upon cooling; As: reverse transformation start temperature upon heating; Af: reverse transformation finish temperature upon heating; T1: the transformation hysteresis.

When the loading-unloading process is finished, the shape memory alloy sample presents a residual strain, which can be recovered by sample heating, which induces the reverse phase transformation. This is the shape memory effect, also known as a one-way shape memory effect. In the case of two-way shape memory effect, the sample has a shape in the austenitic state and another in the martensitic state. In order to obtain the two-way effect, it is necessary that the shape memory alloy sample be trained (TARNIȚĂ *et.al.*, 2009).

Many efforts have been aimed at improving the mechanical properties of biomedical devices. for example, (Zheng *et.al.*, 2013) reviewed how to change surface chemical and physical properties in order to manipulate cell adhesion and behavior. (Tyau *et.al.*, 2015) made surface modification of TiNi-based shape memory alloys by dry

electrical discharge machining .(Chang *et.al.*, 2016) improved mechanical properties by Ultrasonic Nanocrystal Surface Modification.

In this study the effect of the powder metallurgy process variables such as compacting stress and sintering cycles on several physical tests such as x-ray diffraction, porosity and apparent density as well as mechanical tests such as microhardness, surface roughness had been studied and the effect of alloying element of yttrium and tantalum on microhardness, surface roughness of NiTi shape memory alloys also studied.

2. Materials and experimental procedure

The powder metallurgy technique had been used to prepare samples of porous NiTi shape memory alloys. The procedure involves mixing of powder, compaction and sintering in specific temperature. The sensitive balance of four digit accuracy had been used to prepare samples in the following proportions illustrated in the below table:

Table1: the alloy code and their compositions prepared in this study.

Alloys code		Chemical compositions (Wt. %)
1	A	55 Ni - 45Ti
2	B1	54 Ni – 45Ti – 1 Y
3	B2	53 Ni – 45Ti – 2 Y
4	B3	52 Ni – 45Ti – 3 Y
5	C1	54 Ni – 45Ti – 1 Ta
6	C2	53 Ni – 45Ti – 2 Ta
7	C3	52 Ni – 45Ti – 3 Ta

These chemical composition mixed for three hours by using planetary ball mixer then compacted by using electric hydraulic press of the uniaxial pressing with several compacting pressure of (400,500,600 and 650) MPa to form cylindrical samples with average diameters (15.2) mm and height of (6) mm had been done in Babylon university college of materials engineering metallurgical department. The sintering process accomplished at two step, the first one at temperature 500 °C for two hours and the second at 850 °C for six hours under vacuum conditions (6.7 E -02 Pa) then the specimens cooled in the furnace had been done in kerballa University College of engineering mechanical department. After sintering all surfaces of each of them were grinded with 180, 220, 320,400,600,800, 1000,1200 and 2000 grit silicon carbide papers, then polished with alumina solution and 3µm diamond paste to get mirror finish appearance. And then washed with distilled water. A dryer was used as manual dryer for drying up the samples and then kept the samples with silica gel in a well- knit cans to keep them completely dry. Then each sample was immersed in etching solution for (8-10) seconds, then washed with distilled water and dried rapidly ,finally microstructure observations carried out for the samples. Etching of samples achieved in solution with chemical composition as the following (Sounia *et.al.*, 2002): (HF 10 ml , HNO3 20ml , H2O 80ml). The hardness of the samples has been measured by using Microhardness Vickers's tester, the applied weight was (200 gm) and the incubation time was (10 sec) in state applied weight .Three measurements for each sample had been taken and the average value used to analysis the behavior of the alloys. A roughness tester model of (TR200) with cut off equals to 1.2(µm) has been used to quickly and accurately determine the surface texture or surface roughness of all samples. A roughness tester

shows the mean roughness value (Ra) in micrometers or microns (μm). All tests had been done in Babylon university college of materials engineering metallurgical department.\

3. Results and discussion

3.1 porosity and apparent density before and after sintering

Figures (2) and (3) shown that the green density of all green samples with the effect of compacting stress.it is clear that the green density increase as the compacting stress increase this attributed to decreasing the pore as the compacting stress increased, however, the pore size and pore distribution will also change.

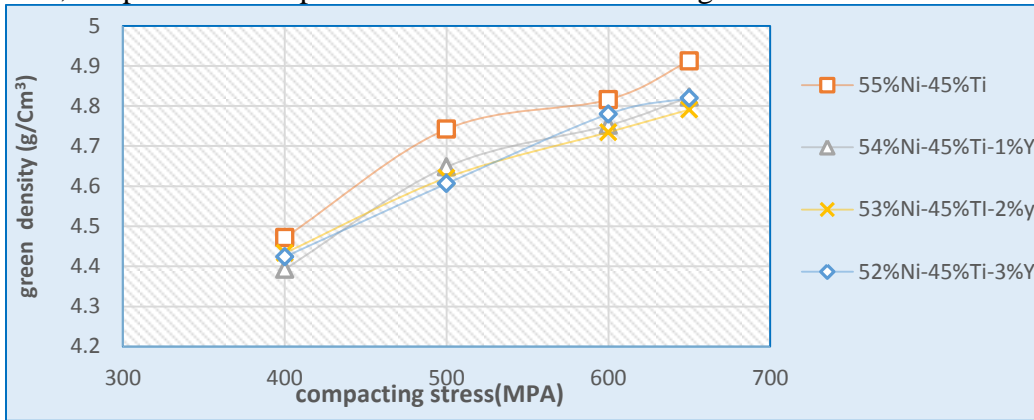


Fig. (2): green density versus compacting stress.

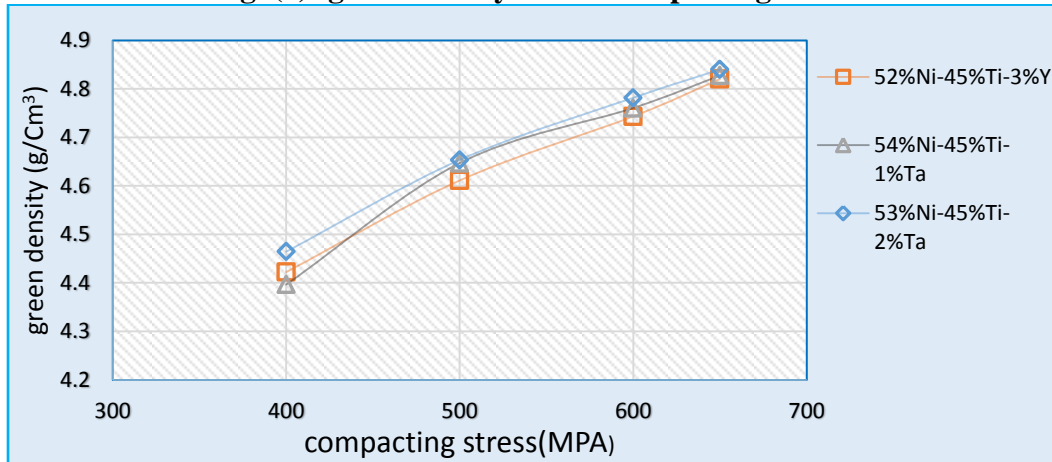


Fig. (3): green density versus compacting stress.

The porosity of green samples against compacting stress also depicted in figure (4) and (5).it has been shown that the porosity decrease as the compacting stress increase. The reason of this is that with increasing of compacting pressure , The density of the powder mass increases, so the total amount of porosity in the mass decreases , however , the pore size and pore distribution will change as well.

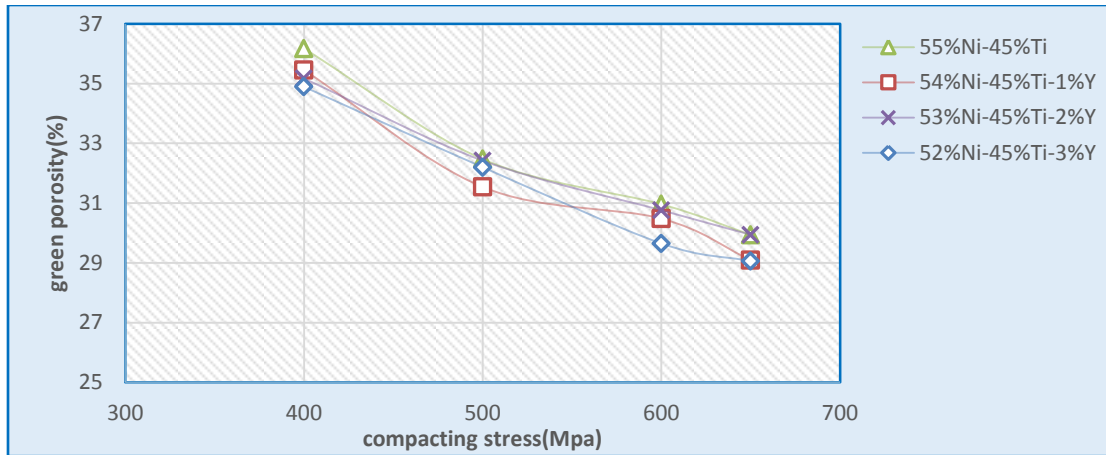


Fig. (4): green porosity versus compacting stress.

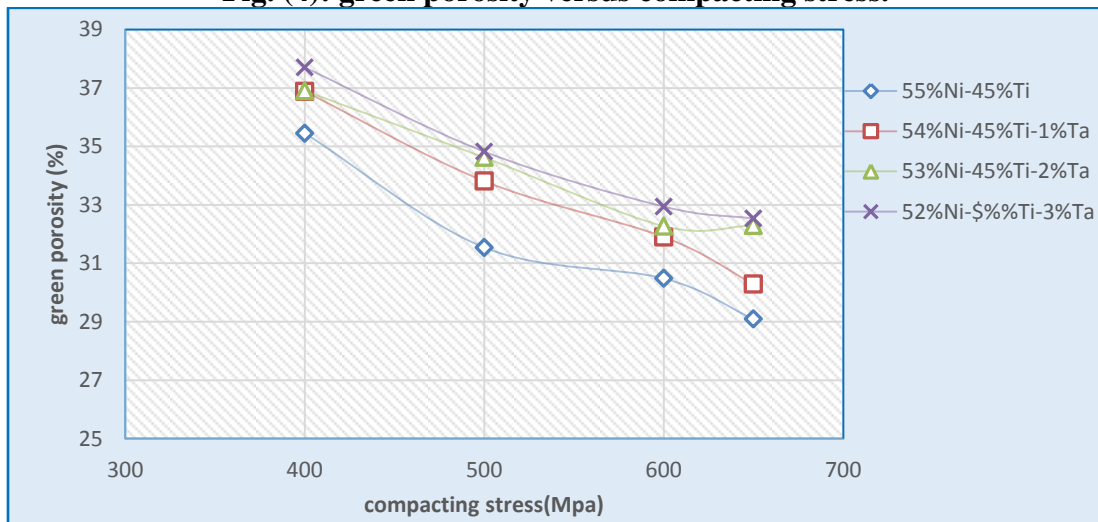


Fig. (5): green porosity versus compacting stress.

The density and porosity of sintered sample showed in below figures (6, 7, 8 and 9), also the density increase as the compacting stress increase while porosity decrease as the compacting stress increase.

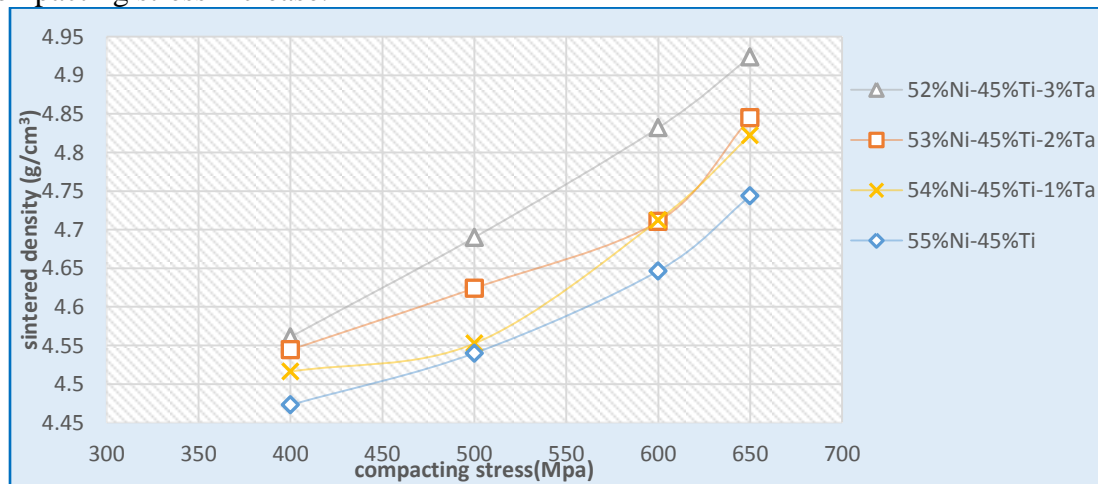


Fig. (6): density of sintered sample vs compacting stress.

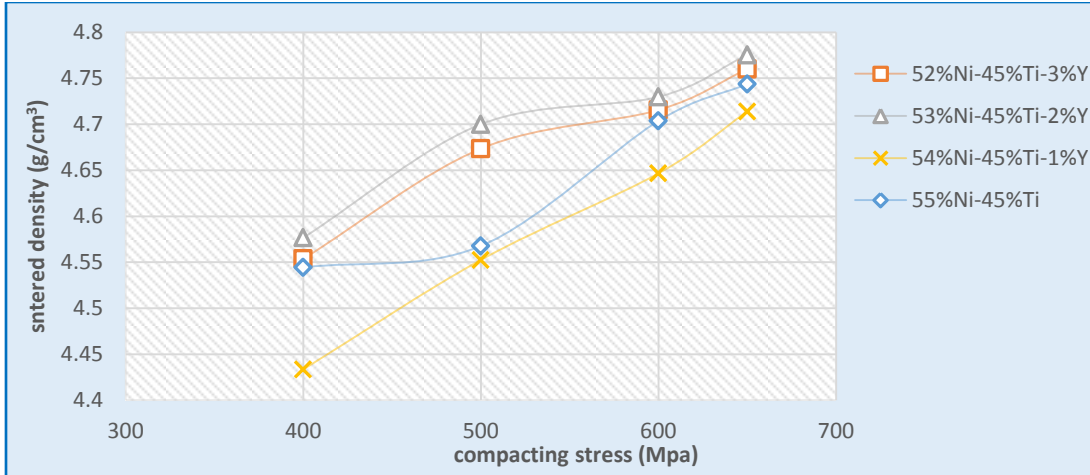


Fig. (7): density of sintered sample vs compacting stress.

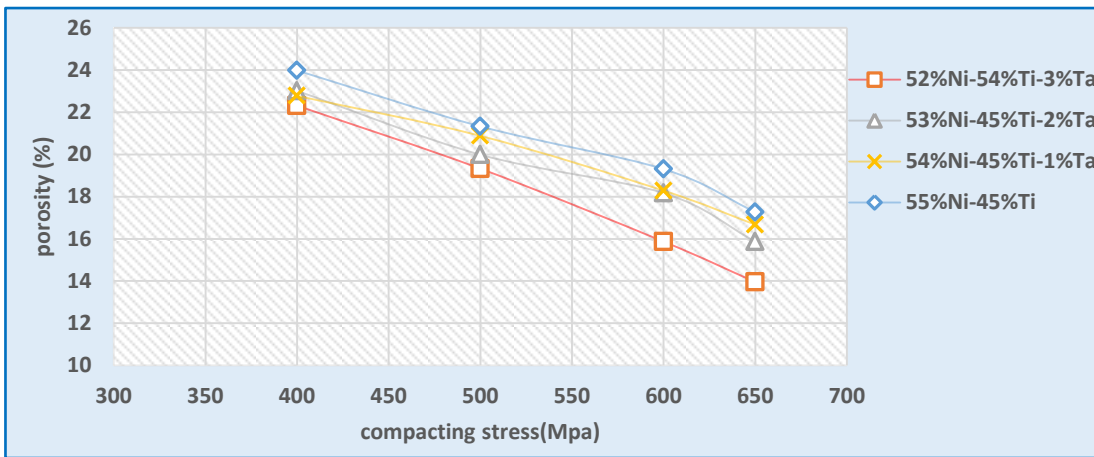


Fig. (8): porosity of sintered sample vs. compacting stress.

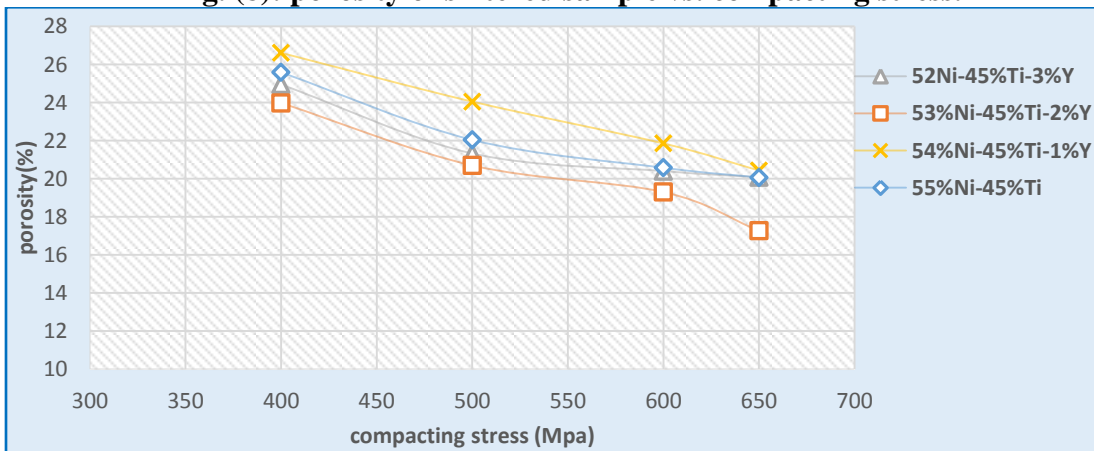


Fig (9): porosity of sintered sample vs. compacting stress.

3.2 X-Ray diffraction (XRD)

It is important to have XRD test to identify the phases of crystalline structure. The test was done for elemental powder of base sample, base alloy after sintering, and B3 and C3 alloys after sintering process. Figure (10) depicted the XRD pattern for NiTi powder, these patterns show only Ni and Ti phases, because no phase transformation occurs

during mixing or compacting process since there is no sufficient heat. These patterns matched the standard patterns for Ni and Ti powders. Figure (11) illustrated the XRD patterns for the base alloy after sintering in accordance with the sintering process mentioned in the experimental procedure under vacuum condition. In this pattern all Ni and Ti transformed to monoclinic NiTi phase and hexagonal Ni₃Ti phase. Figure (12) and (13) depicted XRD pattern for B3 and C3 alloys after sintering process which shows also the same pattern for base alloys after sintering process this means that additives have not led to the occurrence of other compounds and this is required.

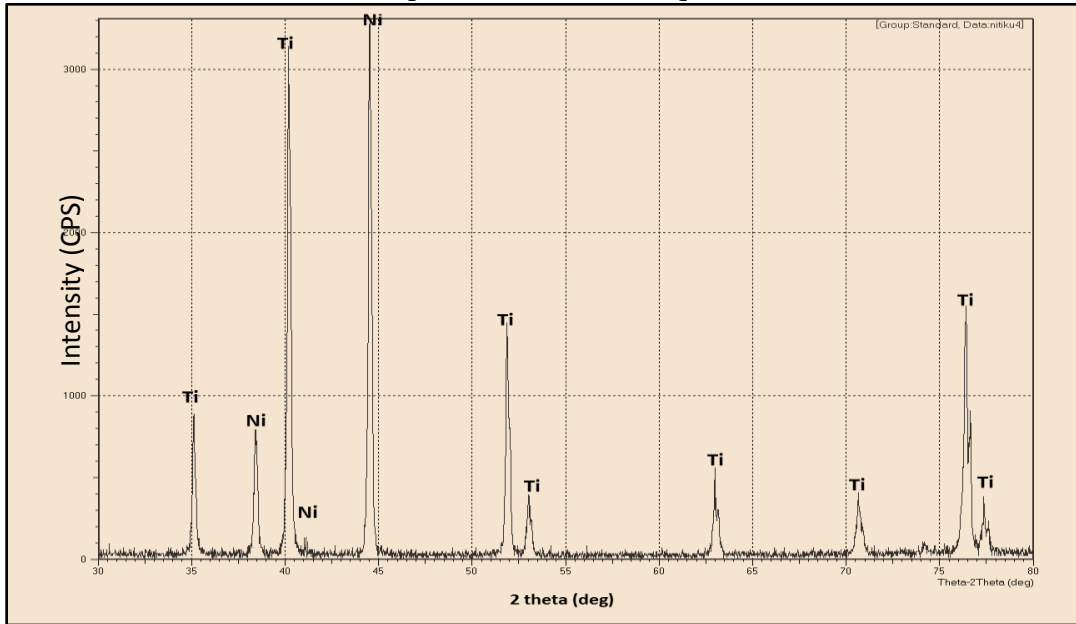


Fig. (10): XRD pattern for NiTi powder.

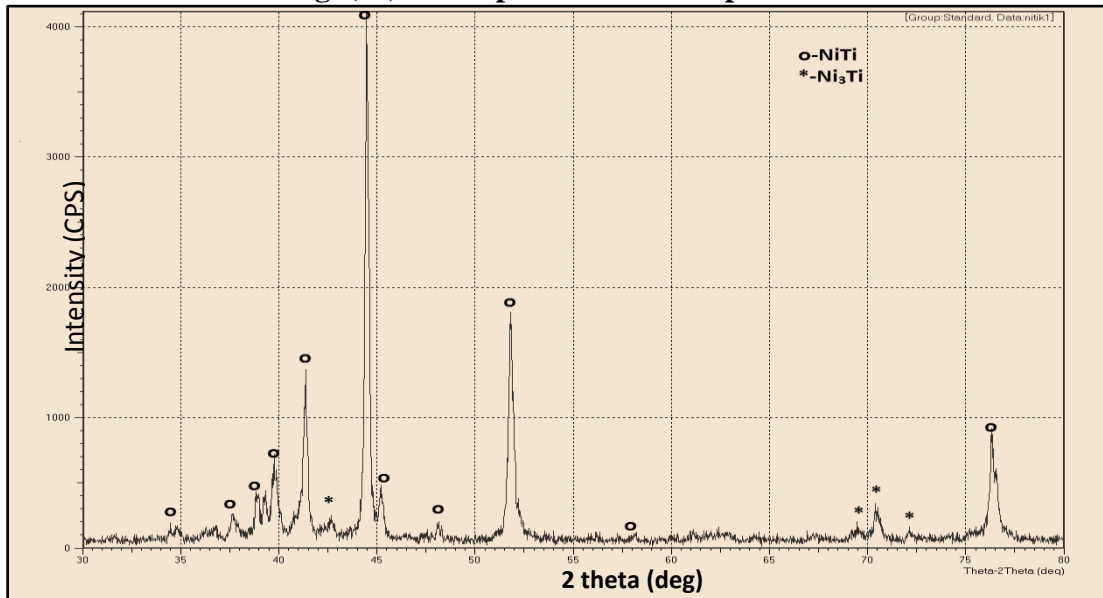


Fig. (11) XRD pattern for base alloys after sintering process.

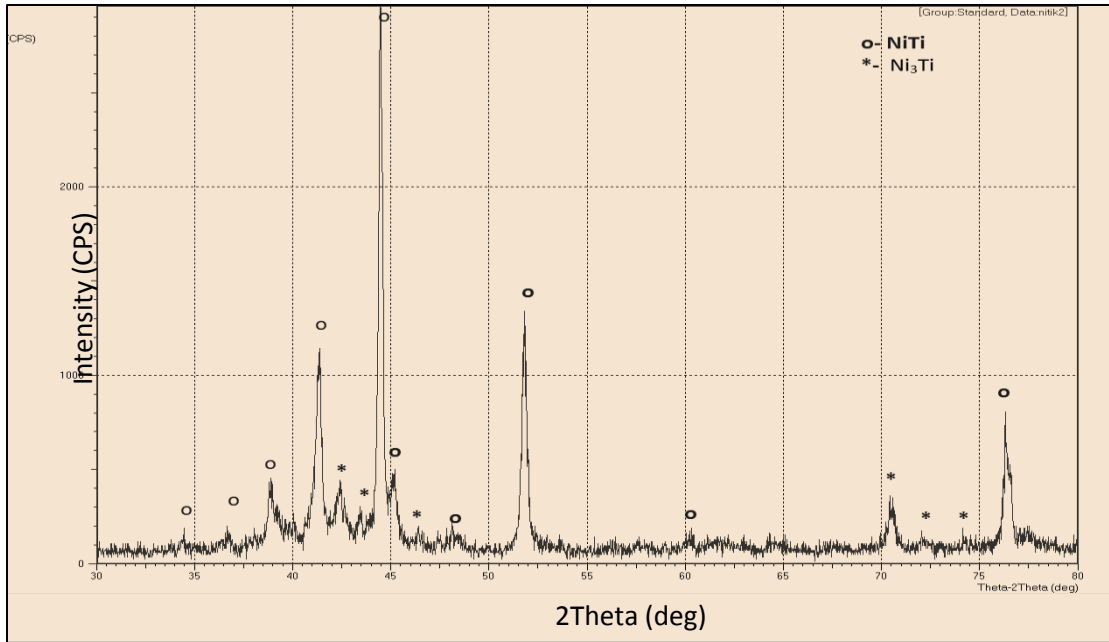


Fig. (12): XRD pattern for B3 alloys.

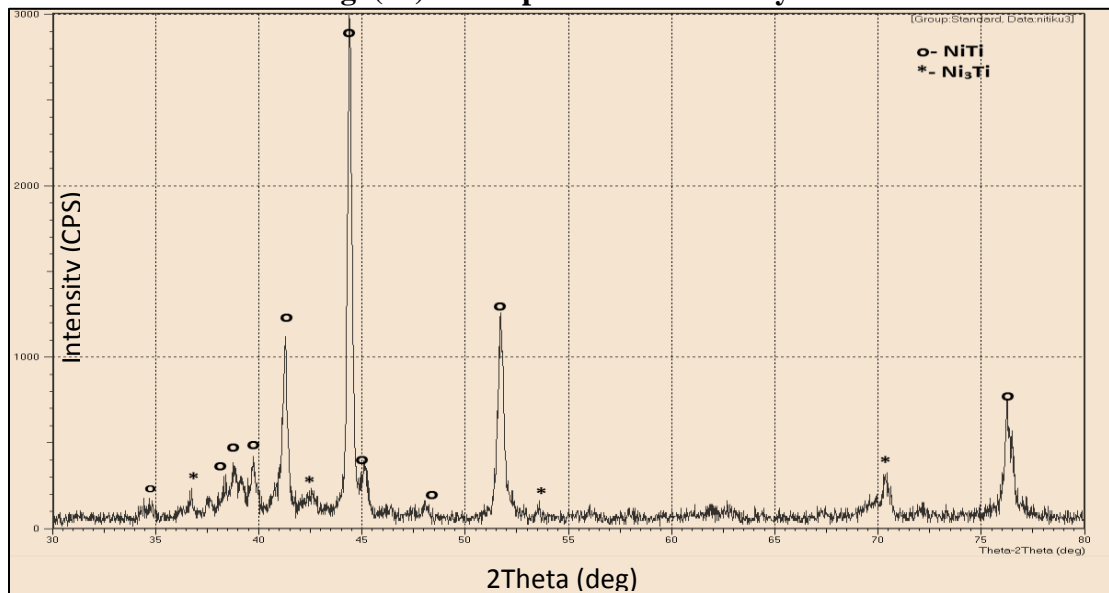


Fig. (.13): XRD pattern for C3 alloys.

3-3 Hardness test results

As seen from Figs. (14) and (15) the hardness value of all sintering samples increase as the compacting stress increase. Fig. (14) shown that the hardness values for NiTi alloys with yttrium additives at 2% Y higher than base alloy while at 1% showed less than base alloys , As well as in Fig. (15), it is clear that the sample with the highest percentage of tantalum additives and compacting stress showed the highest hardness values since the tantalum alloy is harder than the yttrium alloy thus the additive of tantalum change the microstructure morphology and made grain boundary increase the hardness of alloys while the addition of yttrium makes the material more ductile by reducing the stress to induce or reorient variants of martensite.

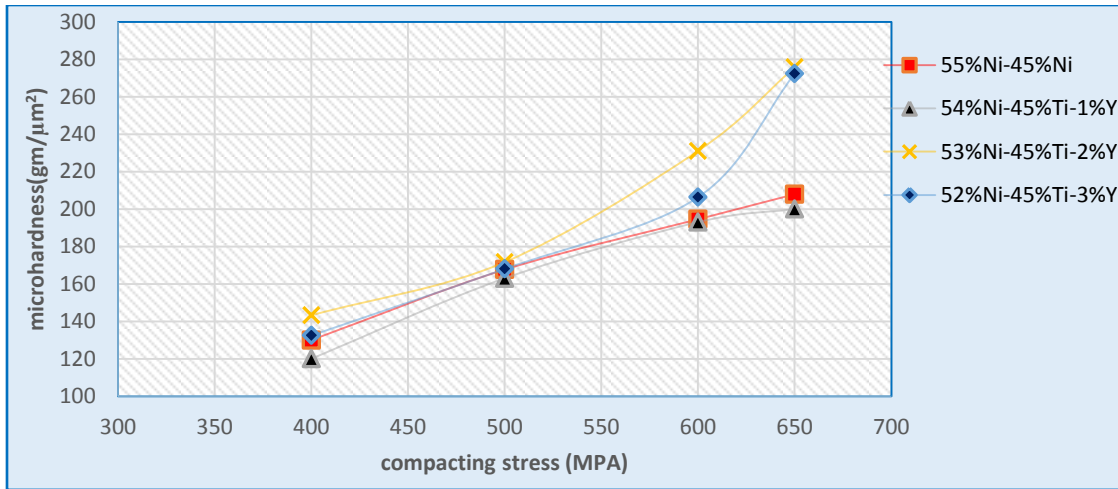


Fig. (14): Hardness values versus compacting stress.

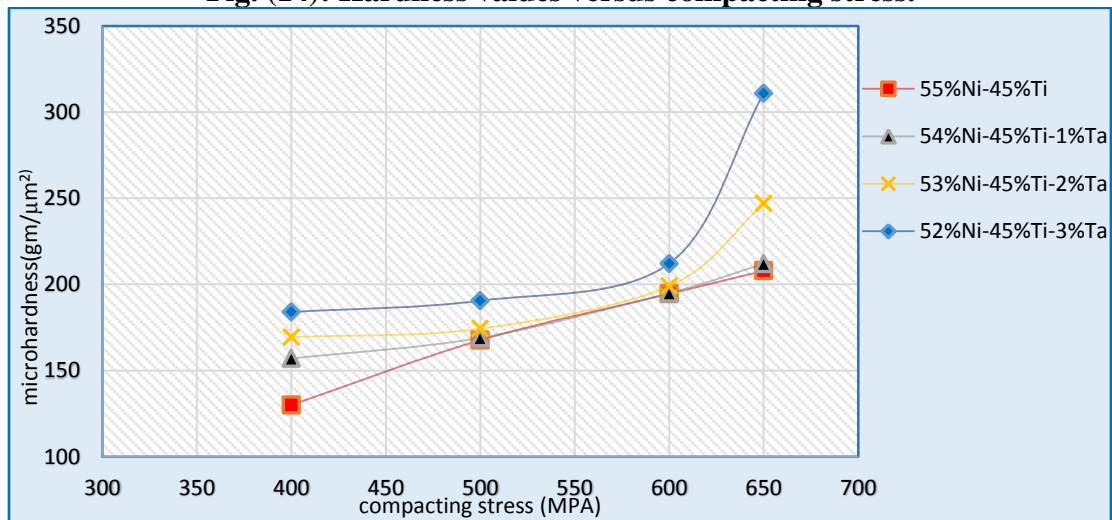


Fig. (15): Hardness values versus compacting stress.

3-4 Surface roughness test results

Surface roughness is a very important property affecting the behavior of mating contact surfaces. In fact low roughness values increase the manufacturing costs, but it is important for knowing the material performance and the contact elements since it has a primary role in Tribology. Actually, rough surfaces tend to wear rapidly and have higher coefficients of friction compared to smooth ones (Hamrock *et.al.*, 2014). Figure (16) shown that the effect of yttrium additives on surface roughness value, it found that the increment of yttrium reduced the surface roughness value, as well as the tantalum additives reduced the surface roughness as the tantalum content increase as seen in figure (17), since the tantalum alloy is the hardest thus the alloys with tantalum additives is better than the alloys with yttrium additives and it is clear from both of figures the surface roughness reduced as the compacting stress increased and this is natural manner because the pores is reduced.

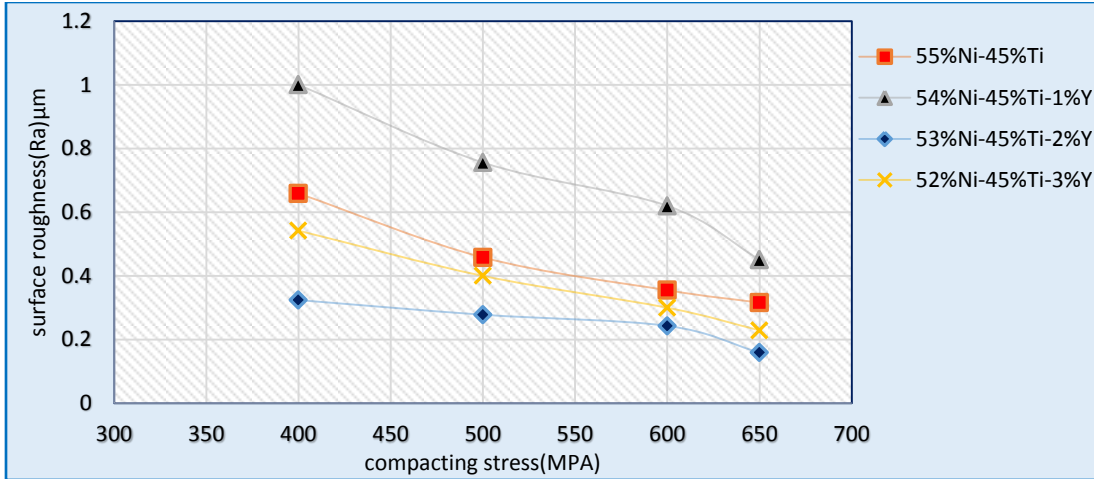


Fig. (16): surface roughness versus compacting stress.

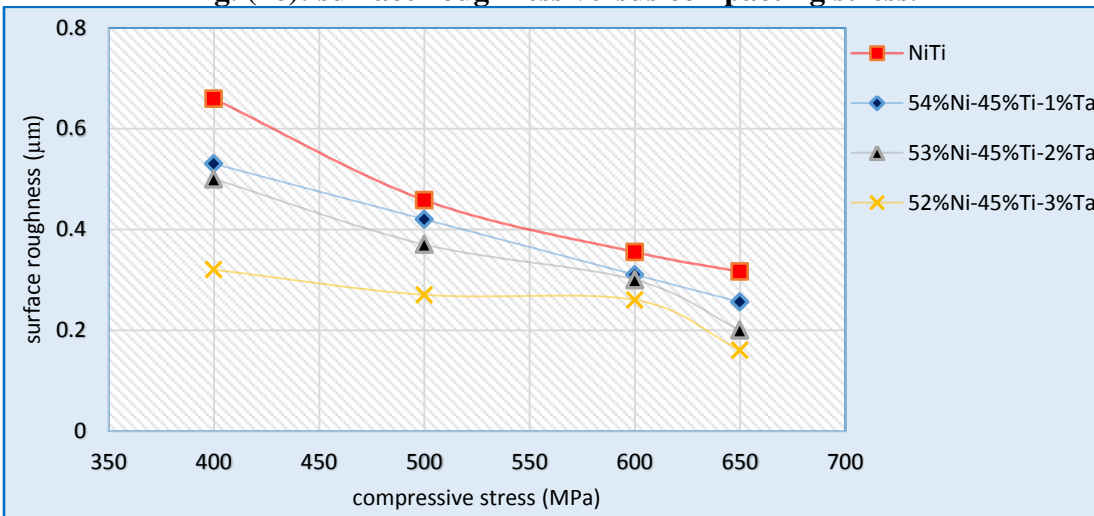


Fig. (17): surface roughness versus compacting stress.

3-5 microstructure analysis (LOM)

The LOM with magnification power of 50 has been done for all sintering samples to illustrate the grain boundaries, pores in different sizes and the present phases, thus many figures were chosen in different compacting stress to illustrate this. Figure (18) illustrated the microstructure of etched B1, C1, C2 and C3 alloys of different compacting stress after the sintering process with 500x. The figures show many pores with different sizes on the surface, that is the true manner since the samples were prepared by powder metallurgy technique.

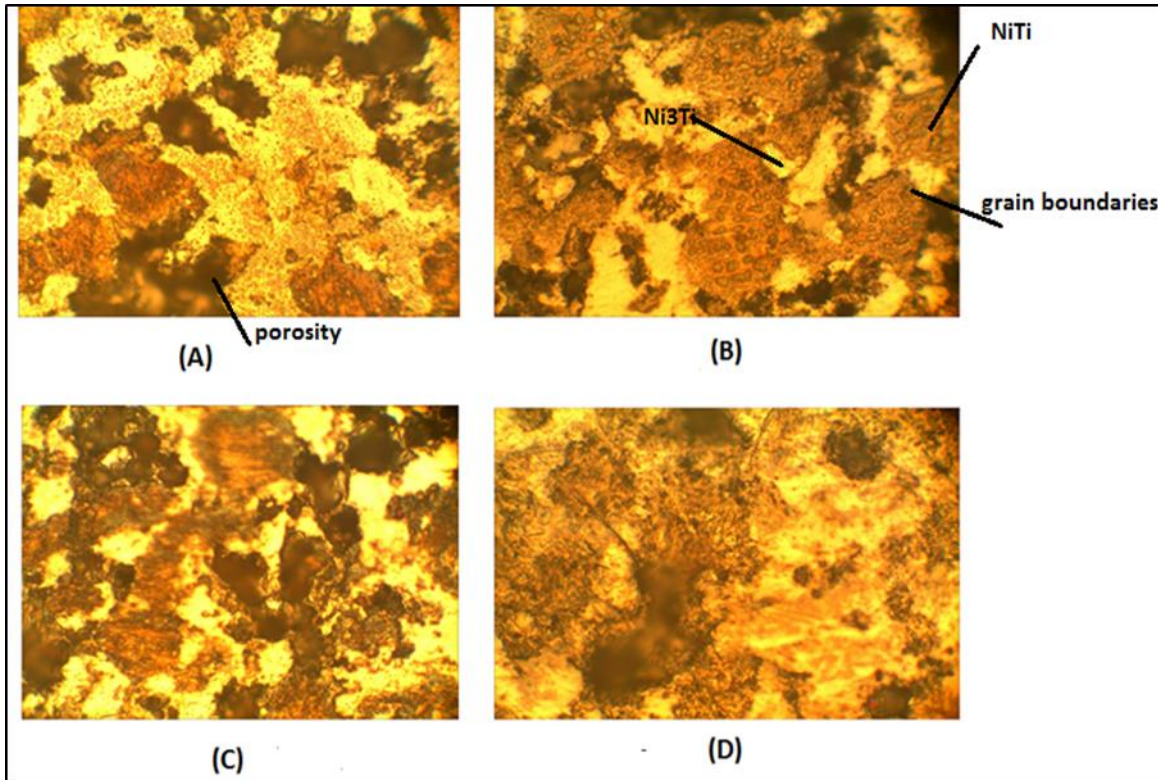


Fig. (18): Microstructure for (A) C1 of 400Mpa, (B) C3 of 500Mpa ,(C) C2 of 600Mpa, (D) B1 of 650 Mpa.

4. Conclusions

1. The sintering at 500 °C for 2h of samples and at 850 C° for 6 h under vacuum condition $6.7 \cdot 10^{-2}$ Mpa is sufficient to complete the transformation process of Ni, Ti, Ta and Y to alloy structure.
2. Two phases structure is appear in all alloys, monoclinic NiTi and hexagonal Ni₃Ti.
3. The alloys with Y additives (1% and 3%) wt. % have hardness values lower than that for NiTi alloy with 2% additives. While, the addition of Ta increase the hardness values as the percentage increase.
4. The addition of Ta decrease the surface roughness as the percentage increase, the alloys with Y additives (1 %and 3%) wt. have surface roughness higher than the alloys with 2% additives.

5. References

- DANIELA TARNIȚĂ, D. N. TARNIȚĂ, N. BÎZDOACĂ, I. MÎNDRILĂ, MIRELA VASILESCU** , 2009 . "Properties and medical applications of shape memory alloys, University of Craiova", Romanian Journal of Morphology and Embryology, 50(1):15–21.
- DUERIG T., PELTON A., STÖCKEL D.** , 1999 , "An overview of nitinol medical applications", Mater Sci Eng A, 273–275:149– 160.
- Es-Sounia M., Es-Sounib M., Fischer-Brandies H.** , 2002 , "On the properties of two binary NiTi shape memory alloys. Effects of surface finish on the corrosion behaviour and in vitro biocompatibility" Biomaterials, Vol. 23, PP. 2887–2894.

- Hamrock B., Jakobson B. and Schmid S.** , 2014 .”Fundamentals of Machine Elements”, Third Edition. New-York: CRC press.
- Mantovani D** , 2000 . “Shape memory alloys: Properties and biomedical applications”.
Journal of the Minerals, Metals and Materials Society, 52: 36-44.
- OTSUKA K., REN X.** , 1999 , “Recent developments on the research of shape memory alloys”, Intermetallics, 7(5):511–528.